

RESEARCH

Open Access



Identification of a novel metabolism-related gene signature associated with the survival of bladder cancer

Xiaotao Li^{1,2,3}, Shi Fu^{1,2,3}, Yinglong Huang^{1,2,3}, Ting Luan^{1,2,3}, Haifeng Wang^{1,2,3*} and Jiansong Wang^{1,2,3*}

Abstract

Background: Bladder cancer (BC) is one of the most common malignancies and has a relatively poor outcome worldwide. In this study, we attempted to construct a novel metabolism-related gene (MRG) signature for predicting the survival probability of BC patients.

Methods: First, differentially expressed MRGs between BC and normal samples were identified and used to construct a protein-protein interaction (PPI) network and perform mutation analysis. Next, univariate Cox regression analysis was utilized to select prognostic genes, and multivariate Cox regression analysis was applied to establish an MRG signature for predicting the survival probability of BC patients. Moreover, Kaplan-Meier (KM) survival analysis and receiver operating characteristic (ROC) analysis were performed to evaluate the predictive capability of the MRG signature. Finally, a nomogram based on the MRG signature was established to better predict the survival of BC.

Results: In the present study, 27 differentially expressed MRGs were identified, most of which presented mutations in BC patients, and LRP1 showed the highest mutation rate. Next, an MRG signature, including MAOB, FASN and LRP1, was established by using univariate and multivariate Cox regression analysis. Furthermore, survival analysis indicated that BC patients in the high-risk group had a dramatically lower survival probability than those in the low-risk group. Finally, Cox regression analysis showed that the risk score was an independent prognostic factor, and a nomogram integrating age, pathological tumor stage and risk score was established and presented good predictive ability.

Conclusion: We successfully constructed a novel MRG signature to predict the prognosis of BC patients, which might contribute to the clinical treatment of BC.

Keywords: Bladder cancer, Metabolism-related gene, TCGA, GEO, Prognosis

Background

Bladder cancer (BC), a malignancy of the urinary tract, is the 10th most prevalent tumor worldwide, with 549,000 newly diagnosed cases and 200,000 deaths estimated in 2018 [1]. It was reported that

urothelial carcinoma accounts for 95% of BC, and most BC patients are nonmuscle-invasive, mainly treated through local treatment or surveillance [2, 3]. However, the clinical treatments of the remaining patients without metastasis primarily rely on surgical resection or a combination of local resection, radiation, and chemotherapy [3]. Although the main therapy for BC patients with unresectable or metastatic disease is platinum-based combination chemotherapies, the survival remains poor, with a median overall survival (OS) of approximately 14 months [4, 5]. On the other

*Correspondence: highphone@126.com; jiansongwangkm@126.com

³ Scientific and Technological Innovation Team of Basic and Clinical Research of Bladder Cancer in Yunnan Universities, The Second Affiliated Hospital of Kunming Medical University, No. 347, Dianmian street, Wuhua District, Kunming 650101, Yunnan, People's Republic of China
Full list of author information is available at the end of the article



hand, even though immune checkpoint blockade has emerged as a novel treatment to extend the OS of some patients, immune checkpoint blockade regrettably does not work in most patients [6]. Therefore, it is essential to recognize novel biomarkers to predict the prognosis and guide the treatment of BC.

Metabolism plays a crucial role in maintaining all biological activities and regulating cell growth and proliferation [7, 8], which has attracted the attention of many researchers in recent years. Cancer cells have unique metabolic characteristics that can satisfy the need for proliferation compared to normal cells [9]. A well-known example of this is the Warburg effect, a unique reprogramming form of glucose metabolism, which can promote the occurrence and development of tumors [10, 11]. On the other hand, the energy demand for meeting the survival of cancer cells in the nutrient-deprived tumor microenvironment relies on metabolic alterations [12]. Recent studies have found that fatty acid metabolism is related to the development of BC [13–15]. Moreover, increasing evidence has revealed that glucose metabolism is also associated with the occurrence and progression of tumors [16, 17]. For example, aberrant expression of miRNA-21 might participate in regulation of the glycolytic phenotype in BC cells [17]. FOXJ1 also has a role in the glycolytic phenotype of BC [18]. Furthermore, the epigenetic perturbation of SAT1 and ASS1 may be involved in the chemotherapy and personalized therapy of BC by regulating its amino acid metabolism [19]. Hence, metabolism plays a vital role in the occurrence and development of BC, and research focusing on metabolism-related genes (MRGs) may contribute to further understanding the role of metabolism in BC and identifying novel therapeutic targets.

Currently, more and more studies have explored the association between MRGs and the prognosis of cancers. For instance, Wen et al. established a model to predict the prognosis of gastric cancer patients based on MRGs [20]. Moreover, a risk model with good performance in the prognostic prediction of hepatocellular carcinoma patients was built based on energy metabolism genes [21]. Wu et al. also found that lipid metabolism-related genes could be used as predictors for the survival of diffuse gliomas [22]. Hence, the present study aimed to establish an MRG signature for predicting the survival of BC based on a series of bioinformatics analyses using the Gene Expression Omnibus (GEO) and The Cancer Genome Atlas (TCGA) databases. Moreover, we further validated the mRNA expression level of genes in the MRG signature through real-time PCR. In brief, the establishment of an MRG signature provided a novel and independent predictor for BC survival and might be conducive to the clinical treatment of BC patients.

Methods

Data collection and processing

The GSE13507 dataset was downloaded from the GEO database, which included 9 healthy controls and 165 patients with BC, and the GSE31684 dataset, which included 93 BC patients with survival information, was extracted from the GEO database as an independent validation set. Moreover, gene expression, somatic mutations and clinical data of 414 BC samples were obtained from the TCGA database, and gene expression data of 19 normal samples were obtained as controls from the TCGA database. Next, we downloaded the gene set (h.all.v7.2.entrez.gmt) from the GSEA website (<https://www.gsea-msigdb.org/gsea/index.jsp>) to screen MRGs by enrichment analysis with the 'clusterProfiler' R package.

Identification of metabolism-related DEGs in BC

The 'DEseq2' R package was selected to identify the differentially expressed genes (DEGs) between normal and BC samples in the TCGA and GEO databases [23]. A P value < 0.05 was regarded as the cutoff criterion. Moreover, two volcano plots were plotted using the 'ggplot2' R package to visualize DEGs in the TCGA and GEO databases [24]. Finally, the metabolism-related DEGs were identified by overlapping the MRGs, DEGs in TCGA and DEGs in GEO using the 'VennDiagram' R package [25].

GO functional annotation and KEGG pathway enrichment analysis

Gene Ontology (GO) functional annotation is an important method to explore the biological process (BP), molecular function (MF), and cellular component (CC) of genes. Moreover, Kyoto Encyclopedia of Genes and Genomes (KEGG) pathway enrichment analysis is a common way to identify gene-related signaling pathways. Therefore, the 'clusterProfiler' R package was utilized to conduct GO functional annotation and KEGG pathway enrichment analysis for the metabolism-related DEGs [26], and a P value < 0.05 was considered to be significantly enriched.

PPI network analysis

To further explore the interactions of the metabolism-related DEGs at the protein level, a protein-protein interaction (PPI) network was built through the Search Tool for the Retrieval of Interacting Genes (STRING, <https://string-db.org/>) website. In addition, Cytoscape was used to visualize the PPI network [27].

Landscape of gene mutations

To further investigate the role of metabolism-related DEGs in BC, the 'maftools' R package was used to analyze the mutation frequency and mutation type of BC

patients from the TCGA database and to draw a waterfall plot showing the landscape of gene mutations for metabolism-related DEGs [28].

Construction and validation of the prognostic MRG signature

To establish and validate the prognostic MRG signature, 383 BC patients (31 patients were removed for subsequent analysis because of a lack of survival information) were randomly divided into a training set and a testing set based on a ratio of 7:3. First, univariate Cox regression analysis was performed using the 'survival' R package to screen the prognosis-related MRGs from the metabolism-related DEGs in the training set, with the a cutoff value of $P < 0.05$. Then, prognosis-related MRGs were submitted to multivariate Cox regression analysis to construct an optimal prognostic MRG signature in the training set by the 'survival' R package. Forest plots were generated to show the results of univariate and multivariate Cox regression analysis by using the 'forestplot' R package. Subsequently, an MRG signature was constructed based on the expression levels and Cox coefficients of the MRGs obtained by multivariate Cox regression analysis. Namely, the formula of the risk score for the MRG signature was defined as follows: $\text{Risk score} = (\text{exp}_{\text{gene } 1} \times \text{Coe}_{\text{gene } 1}) + (\text{exp}_{\text{gene } 2} \times \text{Coe}_{\text{gene } 2}) + \dots + (\text{exp}_{\text{gene } n} \times \text{Coe}_{\text{gene } n})$. Thus, BC patients in the training set, testing set and validation set were stratified into the high-risk and low-risk groups based on the median risk score value of the MRG signature. Moreover, the Kaplan-Meier (KM) survival curves were drawn by the 'survminer' R package to reveal the OS for patients in the high-risk and low-risk groups, and the log-rank test was used to analyze significant differences in OS. Receiver operating characteristic (ROC) curves were plotted to assess the prediction accuracy of the MRG signature and the area under the curve (AUC) for 1-year, 3-year and 5-year OS was calculated through the 'survivalROC' R package [29].

Association between the MRG signature and clinicopathological features

The association between the MRG signature and clinicopathological features, including gender, age, pathological tumor stage, pathological T stage, pathological M stage, pathological N stage, was calculated by t test in the training set, and $P < 0.05$ was considered statistically significant. In addition, a cluster heatmap was drawn to show the distribution trends of gender, age, pathological tumor stage, pathological T stage, pathological M stage, and pathological N stage between the low-risk and high-risk groups in the training set.

Construction of predictive nomogram

The MRG signature and clinicopathological features were used to identify independent prognostic factors with univariate and multivariate Cox regression analyses in the training set, and the results of univariate and multivariate Cox regression analyses are by forest plots. Next, a nomogram was constructed by independent prognostic factors through the 'rms' R package [30]. Moreover, calibration plot was plotted to assess the predictive ability of the nomogram.

Quantitative real time PCR validation

To further analyze the roles of genes in the MRG signature, we first examined the expression levels of genes in the MRG signature in the TCGA and GEO databases. Next, we collected 10 cancer tissues and 10 pericarcinomatous tissues from BC patients in The Second Affiliated Hospital of Kunming Medical University. Informed consent was obtained from all participating individuals. The study was approved by the Ethics Committee at The Second Affiliated Hospital of Kunming Medical University.

Total RNA from the 20 samples was extracted by TRIzol-A+ Reagent (TIANGEN) based on the manufacturer's guidance. Then, the RNAs were reverse-transcribed into complementary DNA (cDNA) using the FastQuant RT Kit (TIANGEN) according to the manufacturer's procedure. Real-time PCR was performed by upeReal PerMix Plus (SYBRGreen) (TIANGEN) and the Applied Biosystems 7500 Real-time PCR System (Applied Biosystems, Inc., Carlsbad, CA, United States). Through the $2^{-\Delta\Delta\text{Ct}}$ method, the relative expression of genes was calculated. GAPDH was used as an internal references. Primer sequences and annealing temperatures are summarized in Table S1.

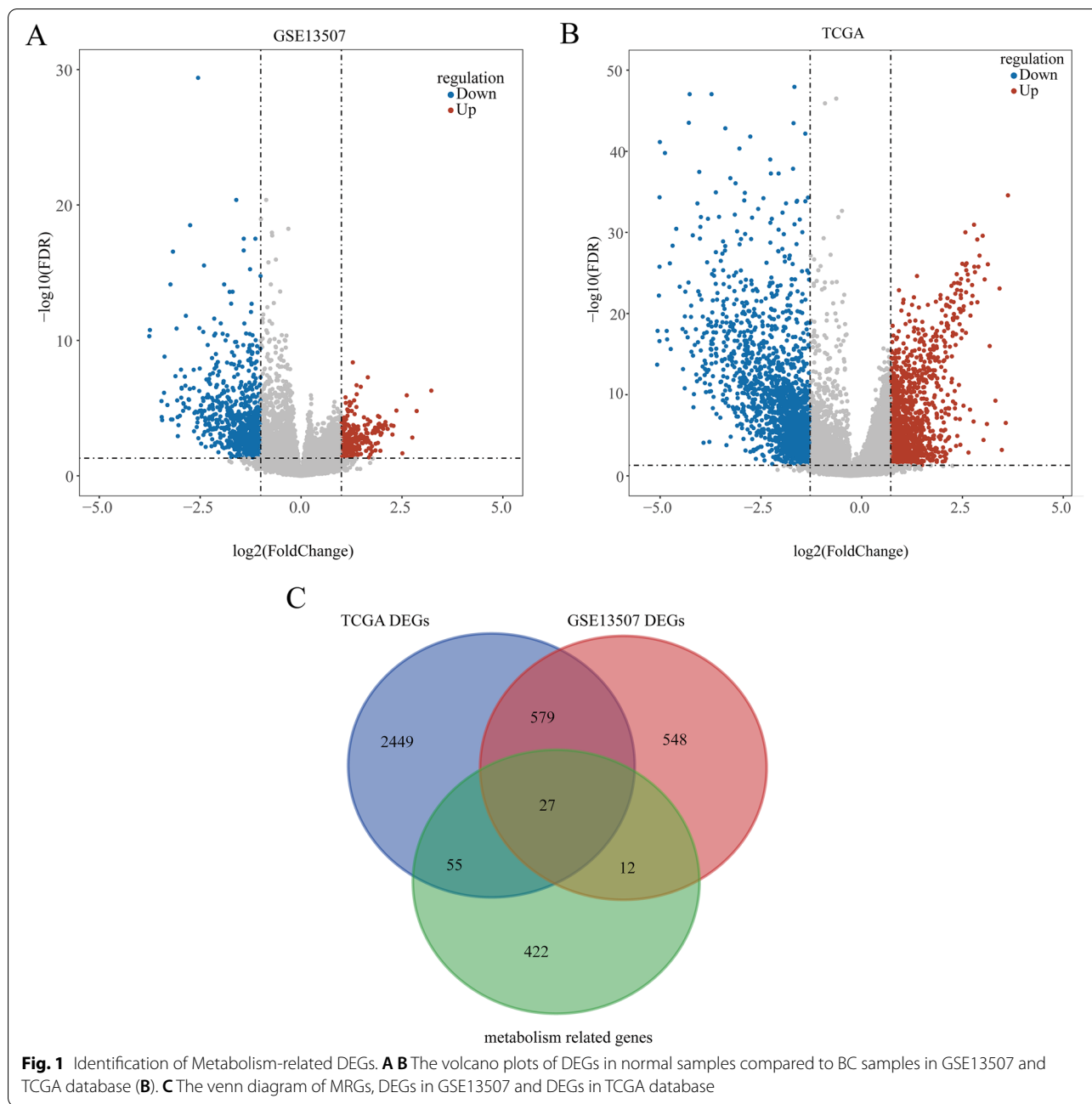
Statistical analysis

All statistical analyses in this study were performed using R software. The differences between different groups were compared by the t test and log-rank test. A P value < 0.05 was considered statistically significant.

Results

Identification of metabolism-related DEGs in BC

We performed functional annotation of the h.all.v7.2.entrez.gmt gene set and obtained 516 MRGs (Table S2). Moreover, under the cutoff of $P < 0.05$, 1166 DEGs, including 288 upregulated genes and 878 downregulated genes, were identified between normal and BC samples in the GEO database (Fig. 1A, Table S3), and 3110 DEGs, including 1306 upregulated genes and 1804 downregulated genes were identified between BC patients and normal samples collected from the TCGA

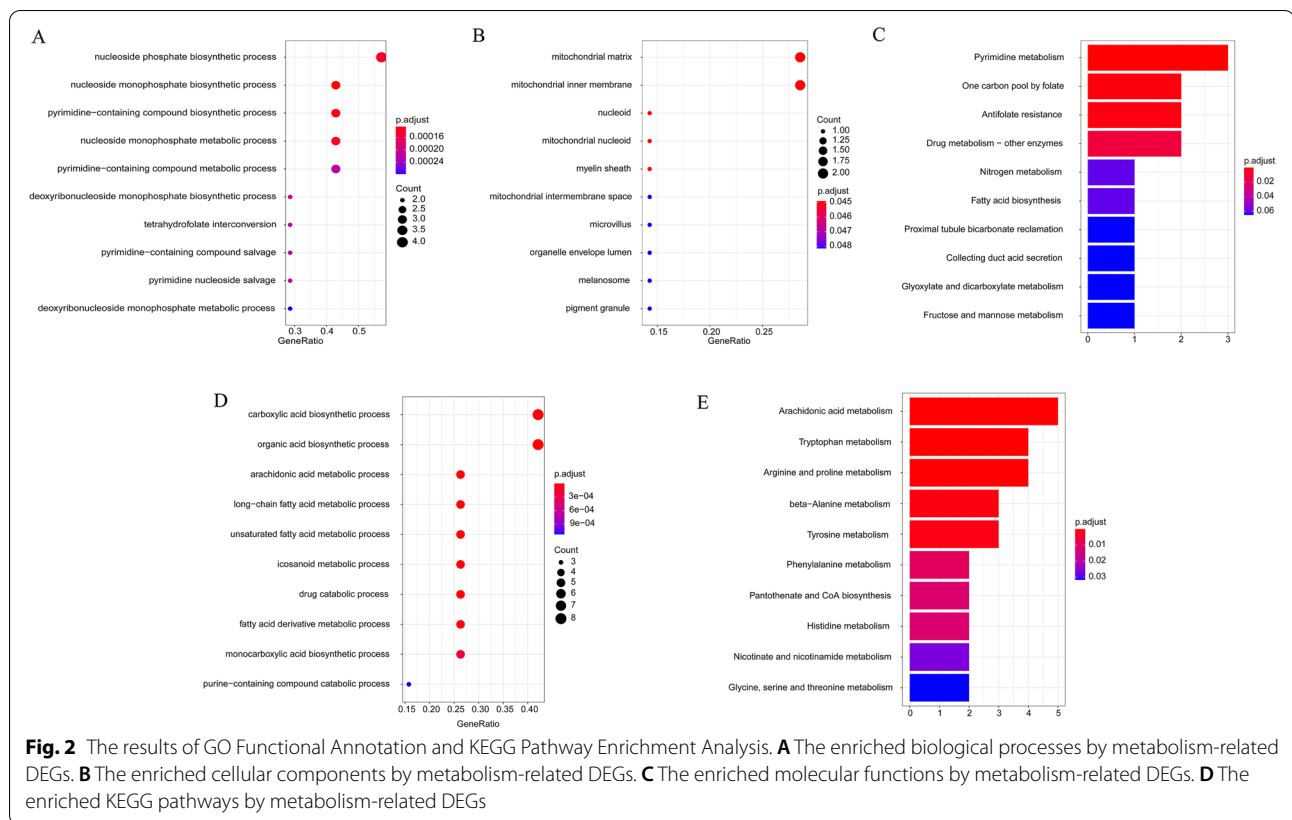


database (Fig. 1B, Table S4). Finally, 27 metabolism-related DEGs were identified, including 19 downregulated and 8 upregulated genes, by overlapping the genes among MRGs, DEGs in GSE13507 and DEGs in the TCGA database (Fig. 1C, Table S5).

GO functional annotation and KEGG pathway enrichment analysis of metabolism-related DEGs

To better understand the biological function of 27 metabolism-related DEGs, we conducted GO function

and KEGG enrichment analyses were conducted. The results of BP for GO analysis showed that 8 upregulated metabolism-related DEGs were primarily associated with biosynthesis and metabolism, for example, nucleoside phosphate biosynthetic process, nucleoside monophosphate biosynthetic process, pyrimidine-containing compound biosynthetic process, nucleoside monophosphate metabolic process, and pyrimidine-containing compound metabolic process (Fig. 2A). For CC analysis, the 8 upregulated metabolism-related DEGs were significantly



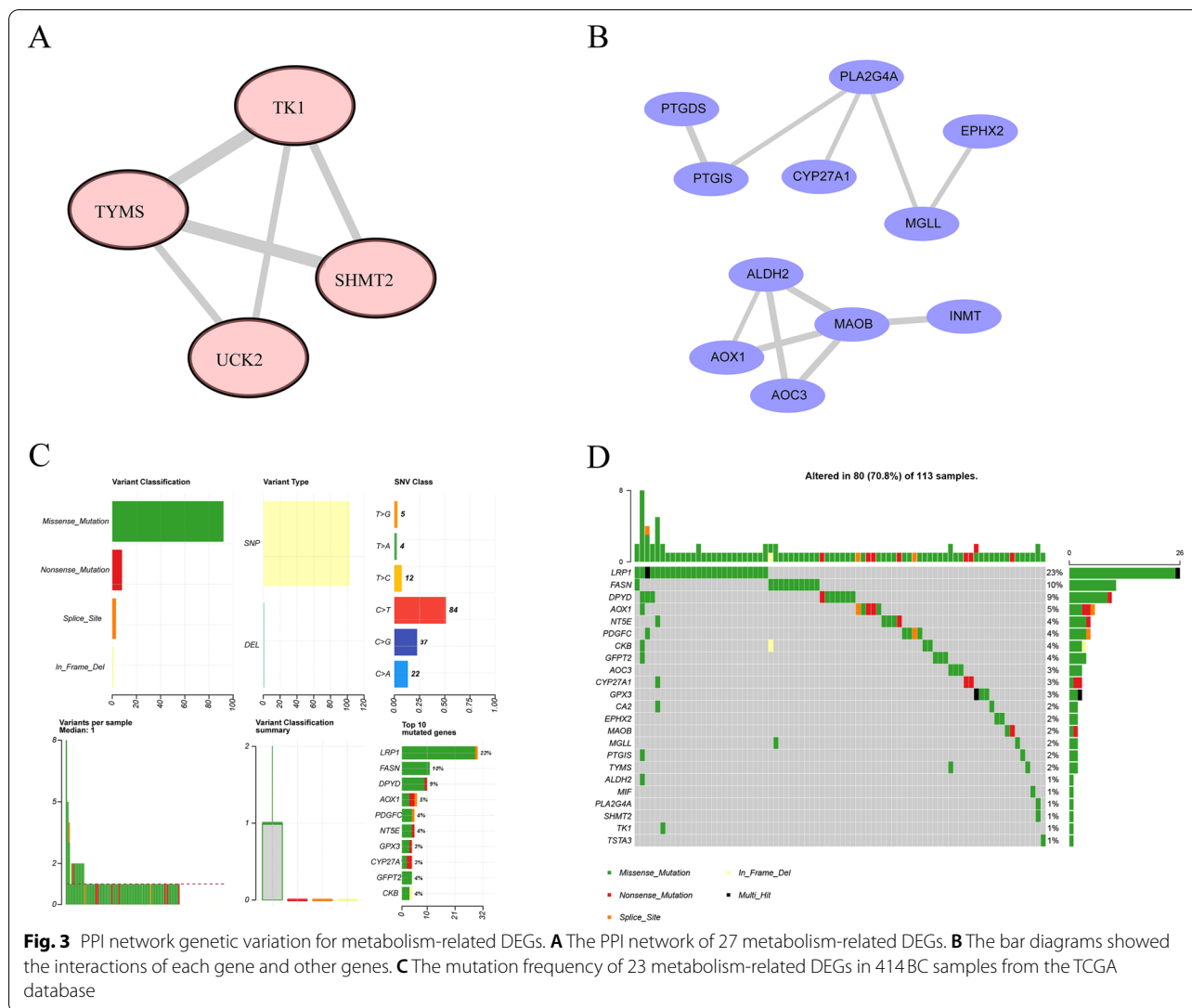
involved in the mitochondrial matrix, mitochondrial inner membrane, and nucleoid (Fig. 2B). In addition, for MF, the 8 upregulated metabolism-related DEGs were not significantly enriched. In particular, KEGG analysis showed that the 8 upregulated metabolism-related DEGs were mainly enriched in metabolism-related pathways, such as pyrimidine metabolism, drug metabolism, nitrogen metabolism, and glyoxylate and dicarboxylate metabolism (Fig. 2C). Similarly, the results of BP for GO analysis showed that the 19 downregulated metabolism-related DEGs were mainly related to biosynthesis and metabolism, such as carboxylic acid biosynthetic process, organic acid biosynthetic process, arachidonic acid metabolic process and long-chain fatty acid metabolic process (Fig. 2D). For CC and MF analysis, the 19 downregulated metabolism-related DEGs were not significantly enriched. Moreover, KEGG analysis showed that the 19 downregulated metabolism-related DEGs were mainly enriched in metabolism-related pathways, such as arachidonic acid metabolism, tryptophan metabolism, arginine and proline metabolism, beta-alanine metabolism, and tyrosine metabolism (Fig. 2E). Thus, these results further suggested that 27 metabolism-related DEGs were mainly related to metabolism-related biological processes and signaling pathways.

PPI network

To further observe the interactions among 27 metabolism-related DEGs, we constructed an up-PPI network and a down-PPI network. As shown in Fig. 3A, upregulated TK1, TYMS, UCK2 and SHMT2 directly interacted with each other. Moreover, downregulated PTGDS, TTGIS, PLA2G4A, CYP27A1, MGLL and EPHX2 directly or indirectly interacted with each other, and ALDH2, AOX1, AOC3, MAOB, and INMT directly or indirectly interacted with each other (Fig. 3B).

Landscape of genetic variation for metabolism-related DEGs

To further investigate the roles of 27 metabolism-related DEGs in the BC, we further analyzed the landscape of somatic mutations for 27 metabolism-related DEGs using somatic mutation data of 414 BC samples from the TCGA database. Notably, among 27 metabolism-related DEGs, most genes experienced mutations in BC patients, and the LRP1 showed the highest mutation frequency (Fig. 3C). Notably, missense was the primary mutation type (Fig. 3C and D). Moreover, the top 10 mutated genes were LRP1, FASN, DPYD, AOX1, PDGFC, NT5E, GPX3, CYP27A1, GFPT2, and CKB (Fig. 3D). In



addition, survival differences were compared between mutated and nonmutated samples of each gene. Interestingly, we found that GPX3 and SHMT2 mutations were related to BC prognosis (*P* value < 0.05, Table S6). These results further revealed that metabolism-related genes might play key roles in BC.

Construction and validation of the prognostic MRG signature

The 383 BC patients were randomly divided into a training set and validation set at a cutoff of 7:3. First, univariate Cox regression analysis identified 5 prognostic MRGs, including PTGIS, MAOB, FASN, LRP1 and SHMT2 (*P* value < 0.05, Fig. 4A), in the training set. Next, 3 genes, MAOB, FASN and LRP1, were reserved to establish a prognostic MRG signature based on the multivariate Cox regression analysis in the training set (Fig. 4B).

MAOB, monoamine oxidase B, an enzyme located on the outer membranes of mitochondria, is responsible for catalyzing monoamine oxidation. FASN, fatty acid synthase, is mainly involved in fatty acid synthesis. LRP1, LDL Receptor Related Protein 1, is associated with several cellular processes, including intracellular signaling, lipid homeostasis, and clearance of apoptotic cells. Notably, all 3 genes were risk factors for BC survival with HR > 1 (Fig. 4B), indicating that higher expression of MAOB, FASN and LRP1 was related to poorer prognosis. Thus, we further plotted the KM survival curves of MAOB, FASN and LRP1 in the training, testing and validation sets and found that patients in the high expression group showed a worse prognosis than patients in the low expression group (Fig. S1). Next, the formula used to calculate the risk score was as follows: Risk score = (0.088 × MAOB expression

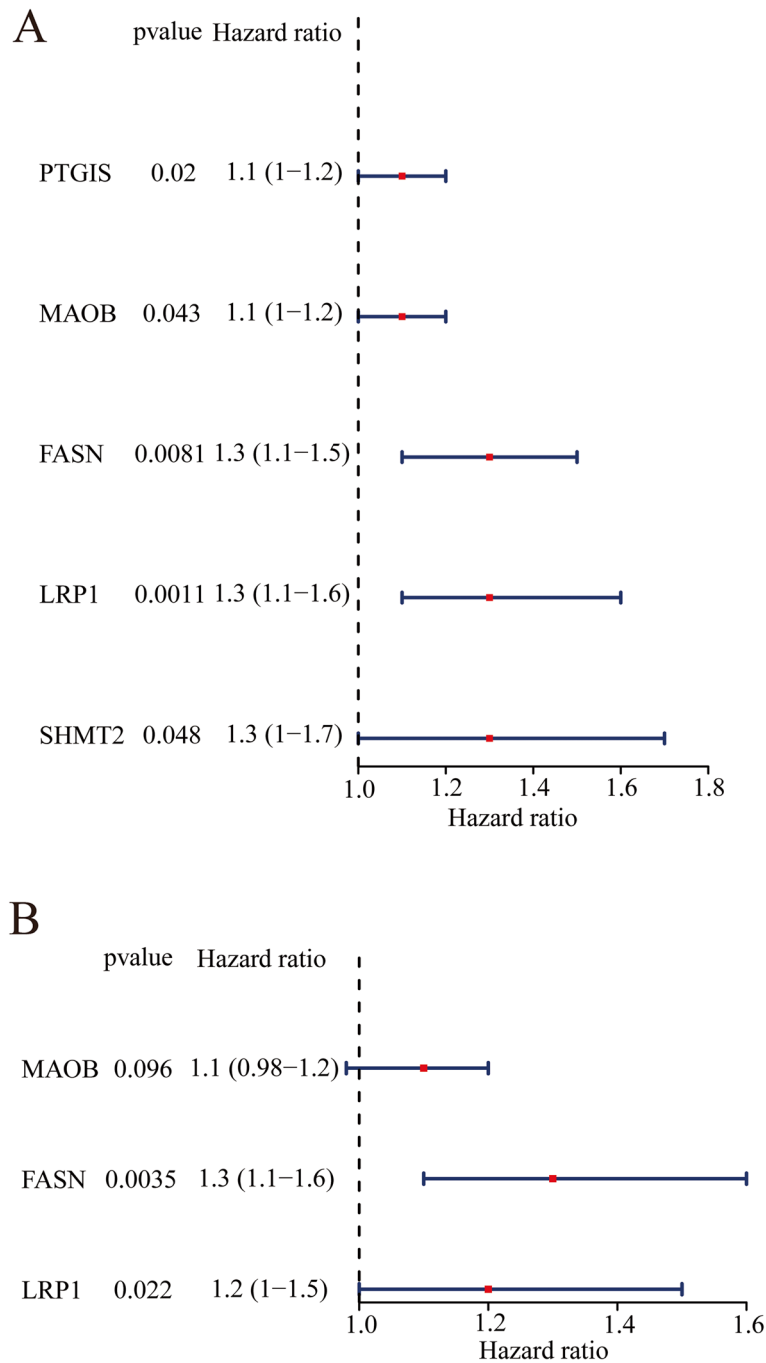
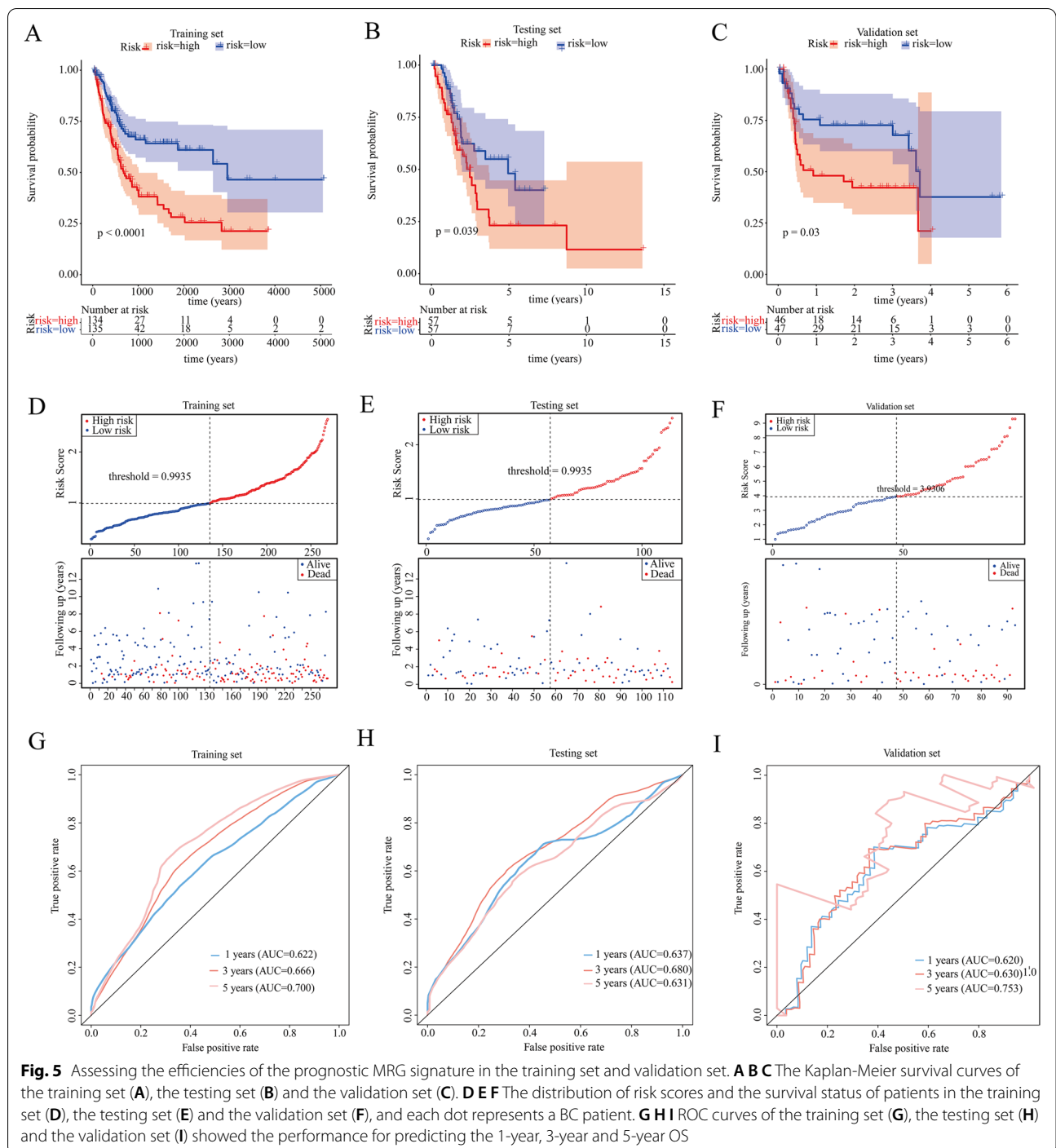


Fig. 4 Identification of prognostic metabolism-related DEGs. **A** Univariate Cox regression analysis identified 5 prognostic metabolism-related DEGs. **B** Multivariate Cox regression analysis reserved 3 prognostic metabolism-related DEGs for establishing the prognostic MRG signature

level) + (0.286 × FASN expression level) + (0.214 × LRP1 expression level). The patients in the training set were stratified into a high-risk group and a low-risk group based on the median risk score value. As shown in Fig. 5A, patients in the high risk group showed significantly poorer OS than those in the low-risk group.

Consistently, the patients in the high-risk group appeared to have a higher mortality than patients in the low-risk group (Fig. 5D). Moreover, the ROC curve suggested that the MRG signature could accurately predict the 1-year, 3-year and 5-year OS, and the AUC values for predicting the 1-year, 3-year and 5-year OS were 0.622, 0.666, and



0.700, respectively (Fig. 5G). Furthermore, based on the formula mentioned above, the patients in the testing set and validation set were stratified into a high-risk group and a low-risk group according to the median risk score value, respectively. Consistent with the results of the training set, the patients in the high-risk group also presented significantly worse OS than those in the low-risk

group in testing set and validation set (Fig. 5B, C, E and F). Similarly, ROC curves of the testing set and validation set also showed better accuracy for predicting the 1-, 3- and 5-year survival of BC patients (Fig. 5H and I), and the AUC values in the testing set were 0.637 at 1 year, 0.680 at 3 years and 0.631 at 5 years (Fig. 5H). Meanwhile, those in the validation set were 0.620, 0.630 and 0.753,

respectively (Fig. 5I). Therefore, these results indicated that the MRG signature presented good performance for predicting the OS of BC patients.

Correlation between the MRG signature and clinicopathological characteristics

To explore the role of the MRG signature in the progression of BC, the association between the MRG signature and clinicopathological characteristics was investigated in the training set. As shown in Table 1, the patients in the high-risk group were inclined to include more patients older than 60. Moreover, the patients in the high-risk group appeared to contain more high-grade BC (including pathological tumor stage 3 and 4) (Table 1). Thus, the gene signature may be associated with the progression of BC, and the expression levels of risk genes might be influenced by the age of patients.

Construction of a nomogram for predicting the OS of BC

To better use the gene signature, a nomogram combining the gene signature and clinical features was established to predict the OS of BC patients. First, univariate and multivariate Cox regression analyses were performed to screen independent prognostic factors in the training set. The results of univariate Cox regression analysis suggested that age, gender, pathological tumor stage, pathological T stage, pathological M stage, pathological N stage and risk score were responsible for the OS of BC (P value < 0.05, Fig. 6A). Next, multivariate Cox regression analysis indicated that age, pathological tumor stage, and risk score could be used to establish a nomogram via the quantitative scoring method (P value < 0.05, Fig. 6B and C). Furthermore, the calibration curve suggested that the nomogram showed good agreement between the predicted OS and observed OS (Fig. 6D). Thus, the nomogram had good accuracy for predicting the 1-year, 3-year and 5-year survival rates of BC patients.

Quantitative real time PCR validation

To further investigate the expression levels of MAOB, LRP1 and FASN, we performed quantitative real-time PCR validation. Notably, the expression levels of both MAOB and LRP1 were downregulated in tumor samples compared with normal samples in the TCGA and GEO databases (Fig. 7A and B), but the expression of FASN was upregulated. Consistent with the TCGA and GEO results, we also found that the expression levels of MAOB and LRP1 were downregulated in cancer tissues compared with paracarcinoma tissues, and the expression of FASN was upregulated (Fig. 7C). Thus, MAOB, LRP1 and FASN might be good biomarkers for BC.

Table 1 Clinicopathological characteristics of patients in high- and low-risk group in the training set

Characteristics	Number	Risk score		P-value
		Low	High	
Total cases	219	109	110	
Gender				
female	44	18	26	0.2520
male	175	91	84	
Age				
>=60	174	80	94	0.0412
<60	45	29	16	
Pathological tumor stage				
1	2	1	1	0.0165
2	60	40	20	
3	79	37	42	
4	78	31	47	
T stage				
T1	2	1	1	0.0629
T2	69	43	26	
T3	117	49	68	
T4	31	16	15	
M stage				
M1	105	46	59	0.2300
M2	108	60	48	
M3	6	3	3	
N stage				
Nx	15	6	9	0.1090
N0	129	74	55	
N1	30	12	18	
N2	41	16	25	
N3	4	1	3	

Discussion

BC is a common malignancy of the urinary tract worldwide and has an approximately three times higher morbidity in men than in women [31, 32]. Although most patients (>70%) have nonmuscle-invasive BC at the initial diagnosis, the high recurrence rate greatly reduces the prognosis of patients and 10–15% of them will eventually progress to the muscle-invasive stage [33–35]. Currently, with the development of surgery, chemotherapy and immunological therapy, the clinical management of BC has undergone major improvement [36, 37]. Nevertheless, the prognosis of BC patients remains poor, and the efficacy of immunological therapy still needs improvement because it only benefits a small proportion of patients [6, 38]. Therefore, screening novel biomarkers to predict the prognosis of BC and treatment remains urgent and challenging. Increasing evidence has revealed that metabolic imbalance can influence the growth, proliferation, angiogenesis, and invasion of cancer cells

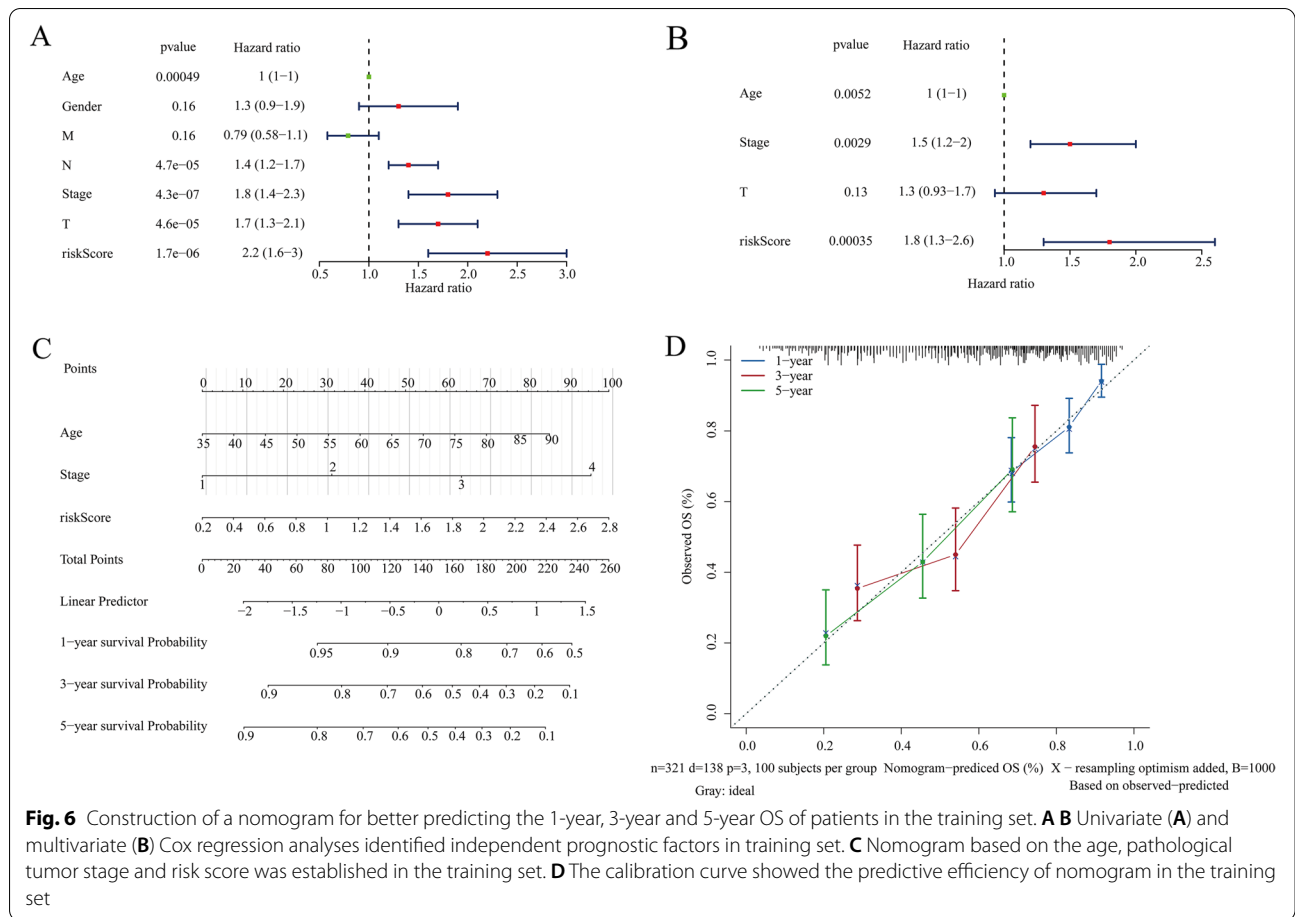


Fig. 6 Construction of a nomogram for better predicting the 1-year, 3-year and 5-year OS of patients in the training set. **AB** Univariate (**A**) and multivariate (**B**) Cox regression analyses identified independent prognostic factors in training set. **C** Nomogram based on the age, pathological tumor stage and risk score was established in the training set. **D** The calibration curve showed the predictive efficiency of nomogram in the training set

[39–41]. Although recent research has revealed that all types of metabolic pathways, including glucose, lipids, amino acids, nucleotides and other pathways, may act as potential prognostic markers of BC [42], few studies have focused on the regulation of metabolism at the molecular level. Hence, the present study aimed to systematically investigate the role of MRGs in the occurrence and progression of BC and screen biomarkers for predicting the OS of BC.

In the present study, we first identified 27 differentially expressed MRGs by overlapping the MRGs, DEGs in TCGA, and DEGs in GEO (Fig. 1C). Next, we investigated the biological functions of these 27 differentially expressed MRGs and found that they were mainly associated with metabolism (Fig. 2). Thus, we speculated that these genes might play key roles in BC by activating or inhibiting metabolism-related pathways, and ultimately affecting the substances and energy which are necessary for tumor cells growth and reproduction of tumor cells. Moreover, we further explored their interactions and genetic changes and found that several genes could interact with each other (Fig. 3A and B), and most genes

experienced mutations in BC patients (Fig. 3C and D). Moreover, an MRG signature with good performance, including MAOB, FASN and LRP1, was established to predict the OS of BC patients. Notably, the gene signature was associated with age and tumor stage (Table 1). Finally, we constructed a nomogram to better use the gene signature and further validated the expression levels of MAOB, FASN and LRP1. Interestingly, the results of quantitative real-time PCR were consistent with the results of TCGA and GEO. Namely, the expression levels of MAOB and LRP1 were downregulated in cancer tissues compared with paracarcinoma tissues, and the expression of FASN was upregulated (Fig. 7).

MAOB, encoding an enzyme that can generate hydrogen peroxide by oxidative reaction, is mainly associated with neurotransmitter metabolism-related biological processes [43]. In the present study, we found that higher expression of MAOB was associated with worse survival in BC patients (Fig. 4B and Fig. S1). Consistent with our results, it has been found that decreasing the mRNA expression level of MAOB can extend the survival time of glioblastoma [44, 45]. In addition, MAOB can be used as

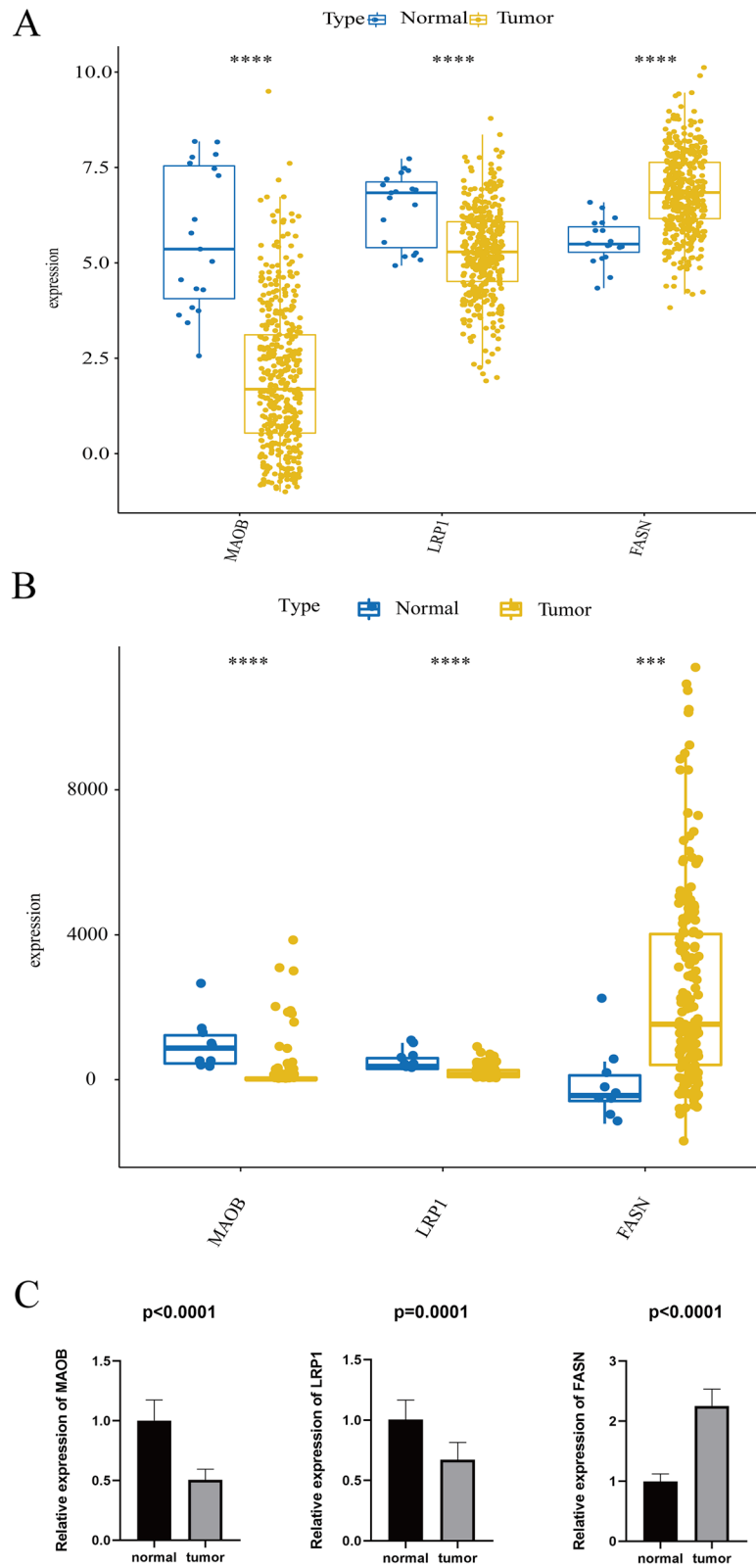


Fig. 7 The expression levels of MAOB, FASN and LRP1. **A** TCGA database. **B** GSE13507. **C** Clinical samples

a novel biomarker to predict the prognosis of colorectal carcinoma [46] and can affect the progression of esophageal cancer [47]. MAOB can also be used as a novel target for the treatment of prostate cancer [48] and presents differential expression in oral tumors [49]. In conclusion, MAOB may be regarded as a biomarker of BC. However, there are no reports about the role of MAOB in BC. Thus, more studies are needed to clarify the role of MAOB in the occurrence and development of BC.

FASN, a key biosynthetic enzyme involved in lipogenesis and the production of longchain fatty acids from acetylcoenzyme A and malonyl-CoA, plays a key role in energy metabolism [50]. It has been regarded as a potential target for the treatment of prostate cancer, thyroid cancer and multiple myeloma [51–53]. Moreover, the expression of FASN is involved in the progression of BC [54]. In particular, FASN has been suggested to be upregulated in BC and to be associated with the histologic grade and recurrence of BC [54, 55], which was consistent with our findings. Moreover, inhibition of FASN expression can suppress the migration capacity of bladder transitional cell carcinoma by activating AKT [56]. Thus, our study further highlights the role of FASN in the occurrence and development of BC.

LRP1, a ubiquitously expressed cell surface receptor, can regulate the lipoprotein metabolism and protease homeostasis [57]. Consistently, LRP1 has been related to the poor prognosis of clear-cell renal cell carcinoma [58]. In addition, LRP1 mutation plays a key role in the occurrence of gastric cancer [59]. It has been demonstrated that the tPA-LRP1 pathway is a key switch for regulating the progression of melanoma by affecting the cellular composition and proteolytic makeup of the tumor niche [60]. More importantly, the expression of LRP1 is involved in the outcome of lung adenocarcinoma [61]. Therefore, LRP1 may be a therapeutic target of BC.

Interestingly, we found that the expression levels of both MAOB and LRP1 were downregulated in BC compared with normal samples, while low expression was associated with prolonged OS (Fig. 7 and Fig. S1). Conversely, FASN was upregulated in BC compared with normal samples, while high expression of FASN was involved in poor OS (Fig. 7 and Fig. S1). Consistent with our research, previous study have revealed that CXCL11 expression is significantly upregulated in colon adenocarcinoma, and upregulation of CXCL11 expression is associated with a better prognosis [62]. Moreover, it was speculated that the paradox between the significance of expression and prognosis for CXCL11 might be due to the regulatory complexity (62). Here, we speculate that MAOB and LRP1 may not affect the occurrence of BC, but may be associated with the development of BC. In brief, BC occurrence may decrease the expression levels

of MAOB and LRP1. Inversely, FASN may be related to the occurrence of BC. However, more research is needed.

Conclusion

In conclusion, based on data from the TCGA and GEO databases, we developed a novel MRG signature to predict the survival of BC. Furthermore, a nomogram integrating the gene signature, age and tumor stage was constructed to preferably predict the survival of BC patients. Moreover, quantitative real-time PCR suggested that the expression levels of MAOB and LRP1 were downregulated in cancer tissues compared with paracarcinoma tissues, and the expression of FASN was upregulated. Therefore, these findings revealed that MAOB, LRP1 and FASN may play key roles in BC by regulating metabolism. However, more research is needed to illustrate their roles in BC.

Abbreviations

BC: Bladder cancer; MRG: Metabolism-related gene; KM: Kaplan-Meier; ROC: Receiver operating characteristic; LRP1: LDL Receptor Related Protein 1; MAOB: Monoamine Oxidase B; FASN: Fatty Acid Synthase; FOXJ1: Forkhead Box J1; SAT1: Spermidine/Spermine N1-Acetyltransferase 1; ASS1: Argininosuccinate Synthase 1; GEO: Gene-Expression Omnibus; TCGA: The Cancer Genome Atlas; GSEA: Gene set enrichment analysis; DEGs: Differentially expressed genes; GO: Gene Ontology; BP: Biological process; MF: Molecular function; CC: Cellular component; KEGG: Kyoto Encyclopedia of Genes and Genomes; PPI: Protein-protein interaction; AUC: Area under curve; cDNA: Complementary DNA; GAPDH: Glyceraldehyde-3-Phosphate Dehydrogenase; TYMS: Thymidylate Synthetase; TK1: Thymidine Kinase 1; DPYD: Dihydropyrimidine Dehydrogenase; UCK2: Uridine-Cytidine Kinase 2; AKT: AKT Serine/Threonine Kinase.

Supplementary Information

The online version contains supplementary material available at <https://doi.org/10.1186/s12885-021-09006-w>.

Additional file 1: Figure S1. The KM survival curves of MAOB, FASN and LRP1 in the training, testing and validation sets. (A) The training set. (B) The testing set (C) The validation set.

Additional file 2: Table S1. The primer sequences and annealing temperatures of MAOB, FASN and LRP1.

Additional file 3: Table S2. The metabolism-related processes and pathways enriched by h.all.v7.2.entrez.gmt gene set.

Additional file 4: Table S3. The DEGs between normal and cancer samples in GSE13507.

Additional file 5: Table S4. The DEGs between normal and cancer samples in TCGA database.

Additional file 5: Table S5. Twenty-seven metabolism-related DEGs.

Additional file 7: Table S6. The survival analysis between mutated and nonmutated samples of each mutated gene among the 27 metabolism-related DEGs.

Acknowledgements

Not applicable.

Authors' contributions

Jiansong Wang and HaiFeng Wang conceived and designed the research. Xiaotao Li obtained and analyzed the data, and drafted the manuscript. Shi Fu,

Yinglong Huang, and Ting Luan participated in the data analysis and determination of analytical method. All authors read, revised manuscript and approved the manuscript for publication.

Funding

This work was supported by Yunnan Provincial Urological Diseases Clinical Medical Center Project, Joint Program of Applied Basic Research of Yunnan Provincial Department of Science and Technology-Kunming Medical University(202001AY070001–214), Scientific Research Fundation of Yunnan Provincial Education Department (grant NO. 2020J0177).

Availability of data and materials

The GSE13507 dataset used in the present study can be found in GEO database (<https://www.ncbi.nlm.nih.gov/geo/>), and the dataset of TCGA (<https://portal.gdc.cancer.gov/>) is available.

Declarations

Ethics approval and consent to participate

Our research was performed in accordance with the Declaration of Helsinki. This study was approved by the Ethics Committee at The Second Affiliated Hospital of Kunming Medical University, and the informed consent was obtained from all participating individuals.

Consent for publication

Not applicable.

Competing interests

The authors declare that they have no competing interests.

Author details

¹Department of Urology, The Second Affiliated Hospital of Kunming Medical University, No. 347, Dianmian street, Wuhua District, Kunming 650101, Yunnan, People's Republic of China. ²Urological disease clinical medical center of yunnan province, The Second Affiliated Hospital of Kunming Medical University, No. 347, Dianmian street, Wuhua District, Kunming 650101, Yunnan, People's Republic of China. ³Scientific and Technological Innovation Team of Basic and Clinical Research of Bladder Cancer in Yunnan Universities, The Second Affiliated Hospital of Kunming Medical University, No. 347, Dianmian street, Wuhua District, Kunming 650101, Yunnan, People's Republic of China.

Received: 2 July 2021 Accepted: 12 November 2021

Published online: 24 November 2021

References

- Bray F, Ferlay J, Soerjomataram I, Siegel RL, Torre LA, Jemal A. Global cancer statistics 2018: GLOBOCAN estimates of incidence and mortality worldwide for 36 cancers in 185 countries. *CA Cancer J Clin*. 2018;68(6):394–424.
- Wu XR. Urothelial tumorigenesis: a tale of divergent pathways. *Nat Rev Cancer*. 2005;5(9):713–25.
- Chang SS, Bochner BH, Chou R, Dreicer R, Kamat AM, Lerner SP, et al. Treatment of nonmetastatic muscle-invasive bladder Cancer: American urological association/American Society of Clinical Oncology/American Society for Radiation Oncology/Society of Urologic Oncology Clinical Practice Guideline Summary. *J Oncol Pract*. 2017;13(9):621–5.
- von der Maase H, Hansen SW, Roberts JT, Dogliotti L, Oliver T, Moore MJ, et al. Gemcitabine and cisplatin versus methotrexate, vinblastine, doxorubicin, and cisplatin in advanced or metastatic bladder cancer: results of a large, randomized, multinational, multicenter, phase III study. *J Clin Oncol*. 2000;18(17):3068–77.
- Sternberg CN, de Mulder P, Schornagel JH, Theodore C, Fossa SD, van Oosterom AT, et al. Seven year update of an EORTC phase III trial of high-dose intensity M-VAC chemotherapy and G-CSF versus classic M-VAC in advanced urothelial tract tumours. *Eur J Cancer*. 2006;42(1):50–4.
- Bellmunt J, de Wit R, Vaughn DJ, Fradet Y, Lee JL, Fong L, et al. Pembrolizumab as second-line therapy for advanced Urothelial carcinoma. *N Engl J Med*. 2017;376(11):1015–26.
- Zhu J, Thompson CB. Metabolic regulation of cell growth and proliferation. *Nat Rev Mol Cell Biol*. 2019;20(7):436–50.
- Widjaja-Adhi MAK, Golczak M. The molecular aspects of absorption and metabolism of carotenoids and retinoids in vertebrates. *Biochim Biophys Acta Mol Cell Biol Lipids*. 1865;2020(11):158571.
- Liu H, Hu YP, Savaraj N, Priebe W, Lampidis TJ. Hypersensitization of tumor cells to glycolytic inhibitors. *Biochemistry*. 2001;40(18):5542–7.
- Wang G, Wang JJ, Guan R, Du L, Gao J, Fu XL. Strategies to target glucose metabolism in tumor microenvironment on Cancer by flavonoids. *Nat Can*. 2017;69(4):534–54.
- Shankaraiah RC, Veronese A, Sabbioni S, Negrini M. Non-coding RNAs in the reprogramming of glucose metabolism in cancer. *Cancer Lett*. 2018;419:167–74.
- Cairns RA, Mak TW. An Alternative Sugar Fuels AML. *Cancer Cell*. 2016;30(5):660–2.
- Putluri N, Shojai A, Vasu VT, Vared SK, Nalluri S, Putluri V, et al. Metabolomic profiling reveals potential markers and bioprocesses altered in bladder cancer progression. *Cancer Res*. 2011;71(24):7376–86.
- von Rundstedt FC, Rajapakshe K, Ma J, Arnold JM, Gohlke J, Putluri V, et al. Integrative pathway analysis of metabolic signature in bladder Cancer: a linkage to the Cancer genome atlas project and prediction of survival. *Urol J*. 2016;195(6):1911–9.
- Piyarathna DWB, Rajendran TM, Putluri V, Vantaku V, Soni T, von Rundstedt FC, et al. Distinct Lipidomic landscapes associated with clinical stages of Urothelial Cancer of the bladder. *Eur Urol Focus*. 2018;4(6):907–15.
- Li Z, Li X, Wu S, Xue M, Chen W. Long non-coding RNA UCA1 promotes glycolysis by upregulating hexokinase 2 through the mTOR-STAT3/micro-RNA143 pathway. *Cancer Sci*. 2014;105(8):951–5.
- Yang X, Cheng Y, Li P, Tao J, Deng X, Zhang X, et al. A lentiviral sponge for miRNA-21 diminishes aerobic glycolysis in bladder cancer T24 cells via the PTEN/PI3K/AKT/mTOR axis. *Tumour Biol*. 2015;36(1):383–91.
- Xian S, Shang D, Kong G, Tian Y. FOXJ1 promotes bladder cancer cell growth and regulates Warburg effect. *Biochem Biophys Res*. 2018;495(1):988–94.
- Yeon A, You S, Kim M, Gupta A, Park MH, Weisenberger DJ, et al. Rewiring of cisplatin-resistant bladder cancer cells through epigenetic regulation of genes involved in amino acid metabolism. *Theranostics*. 2018;8(16):4520–34.
- Wen F, Huang J, Lu X, Huang W, Wang Y, Bai Y, et al. Identification and prognostic value of metabolism-related genes in gastric cancer. *Aging*. 2020;12(17):17647–61.
- Chen Q, Li F, Gao Y, Xu G, Liang L, Xu J. Identification of energy metabolism genes for the prediction of survival in hepatocellular carcinoma. *Front Oncol*. 2020;10:1210.
- Wu F, Zhao Z, Chai RC, Liu YQ, Li GZ, Jiang HY, et al. Prognostic power of a lipid metabolism gene panel for diffuse gliomas. *J Cell Mol Med*. 2019;23(11):7741–8.
- Love MI, Huber W, Anders S. Moderated estimation of fold change and dispersion for RNA-seq data with DESeq2. *Genome Biol*. 2014;15(12):550.
- Wickham H. *ggplot2: elegant graphics for data analysis*. New York: Springer; 2016.
- Chen H, Boutros PC. VennDiagram: a package for the generation of highly-customizable Venn and Euler diagrams in R. *BMC Bioinformatics*. 2011;12:35.
- Yu G, Wang LG, Han Y, He QY. clusterProfiler: an R package for comparing biological themes among gene clusters. *OMICS*. 2012;16(5):284–7.
- Shannon P, Markiel A, Ozier O, Baliga NS, Wang JT, Ramage D, et al. Cytoscape: a software environment for integrated models of biomolecular interaction networks. *Genome Res*. 2003;13(11):2498–504.
- Mayakonda A, Lin DC, Assenov Y, Plass C, Koeffler HP. Maftools: efficient and comprehensive analysis of somatic variants in cancer. *Genome Res*. 2018;28(11):1747–56.
- Heagerty PJ, Zheng Y. Survival model predictive accuracy and ROC curves. *Biometrics*. 2005;61(1):92–105.
- Iasonos A, Schrag D, Raj GV, Panageas KS. How to build and interpret a nomogram for cancer prognosis. *J Clin Oncol*. 2008;26(8):1364–70.
- Antoni S, Ferlay J, Soerjomataram I, Znaor A, Jemal A, Bray F. Bladder Cancer incidence and mortality: a global overview and recent trends. *Eur Urol*. 2017;71(1):96–108.
- Siegel RL, Miller KD, Jemal A. Cancer statistics, 2019. *CA Cancer J Clin*. 2019;69(1):7–34.

33. Millán-Rodríguez F, Chéchile-Toniolo G, Salvador-Bayarri J, Palou J, Vicente-Rodríguez J. Multivariate analysis of the prognostic factors of primary superficial bladder cancer. *Urol J*. 2000;163(1):73–8.
34. Soukup V, Čapoun O, Cohen D, Hernández V, Babjuk M, Burger M, et al. Prognostic performance and reproducibility of the 1973 and 2004/2016 World Health Organization grading classification Systems in non-muscle-invasive Bladder Cancer: a European Association of Urology non-muscle-invasive bladder Cancer guidelines panel systematic review. *Eur Urol*. 2017;72(5):801–13.
35. van Rhijn BW, Burger M, Lotan Y, Solsona E, Stief CG, Sylvester RJ, et al. Recurrence and progression of disease in non-muscle-invasive bladder cancer: from epidemiology to treatment strategy. *Eur Urol*. 2009;56(3):430–42.
36. Jordan B, Meeks JJ. T1 bladder cancer: current considerations for diagnosis and management. *Nat Rev Urol*. 2019;16(1):23–4.
37. Balar AV, Galsky MD, Rosenberg JE, Powles T, Petrylak DP, Bellmunt J, et al. Atezolizumab as first-line treatment in cisplatin-ineligible patients with locally advanced and metastatic urothelial carcinoma: a single-arm, multicentre, phase 2 trial. *Lancet*. 2017;389(10064):67–76.
38. Yi M, Jiao D, Xu H, Liu Q, Zhao W, Han X, et al. Biomarkers for predicting efficacy of PD-1/PD-L1 inhibitors. *Mol Cancer*. 2018;17(1):129.
39. Hanahan D, Weinberg RA. Hallmarks of cancer: the next generation. *Cell*. 2011;144(5):646–74.
40. Crunkhorn S. Targeting cancer cell metabolism in glioblastoma. *Nat Rev Cancer*. 2019;19(5):250.
41. Rosario SR, Long MD, Affronti HC, Rowsam AM, Eng KH, Smiraglia DJ. Pan-cancer analysis of transcriptional metabolic dysregulation using the Cancer genome atlas. *Nat Commun*. 2018;9(1):5330.
42. Cheng Y, Yang X, Deng X, Zhang X, Li P, Tao J, et al. Metabolomics in bladder cancer: a systematic review. *Int J Clin Exp Med*. 2015;8(7):11052–63.
43. Edmondson DE. Hydrogen peroxide produced by mitochondrial monoamine oxidase catalysis: biological implications. *Curr Pharm Des*. 2014;20(2):155–60.
44. Gerber NK, Goenka A, Turcan S, Reyngold M, Makarov V, Kannan K, et al. Transcriptional diversity of long-term glioblastoma survivors. *Neuro-Oncology*. 2014;16(9):1186–95.
45. Colman H, Zhang L, Sulman EP, McDonald JM, Shooshtari NL, Rivera A, et al. A multigene predictor of outcome in glioblastoma. *Neuro-Oncology*. 2010;12(1):49–57.
46. Yang YC, Chien MH, Lai TC, Su CY, Jan YH, Hsiao M, et al. Monoamine oxidase B expression correlates with a poor prognosis in colorectal Cancer patients and is significantly associated with epithelial-to-Mesenchymal transition-related gene signatures. *Int J Mol Sci*. 2020;21(8):2813.
47. Weng L, Shen S, Wu S, Yin X, Liu B, Shang M, et al. Identification of critical genes and proteins for stent restenosis induced by esophageal benign hyperplasia in esophageal Cancer. *Front Genet*. 2020;11:563954.
48. Xu N, Wu YP, Ke ZB, Liang YC, Cai H, Su WT, et al. Identification of key DNA methylation-driven genes in prostate adenocarcinoma: an integrative analysis of TCGA methylation data. *J Transl Med*. 2019;17(1):311.
49. Russo A, Biselli-Chicote PM, Kawasaki-Oyama RS, Castanhole-Nunes MMU, Maniglia JV, de Santi ND, et al. Differential expression of prostaglandin I2 synthase associated with Arachidonic acid pathway in the Oral squamous cell carcinoma. *J Oncol Pract*. 2018;2018:6301980.
50. Kuhajda FP, Jenner K, Wood FD, Hennigar RA, Jacobs LB, Dick DJ, et al. Fatty acid synthesis: a potential selective target for antineoplastic therapy. *Proc Natl Acad Sci U S A*. 1994;91(14):6379–83.
51. Mansour M, Schwartz D, Judd R, Akingbemi B, Braden T, Morrison E, et al. Thiazolidinediones/PPAR γ agonists and fatty acid synthase inhibitors as an experimental combination therapy for prostate cancer. *Int J Oncol*. 2011;38(2):537–46.
52. Uddin S, Siraj AK, Al-Rasheed M, Ahmed M, Bu R, Myers JN, et al. Fatty acid synthase and AKT pathway signaling in a subset of papillary thyroid cancers. *J Clin Endocrinol Metab*. 2008;93(10):4088–97.
53. Okawa Y, Hideshima T, Ikeda H, Raje N, Vallet S, Kiziltepe T, et al. Fatty acid synthase is a novel therapeutic target in multiple myeloma. *Br J Haematol*. 2008;141(5):659–71.
54. Visca P, Sebastiani V, Pizer ES, Botti C, De Carli P, Filippi S, et al. Immunohistochemical expression and prognostic significance of FAS and GLUT1 in bladder carcinoma. *Anticancer Res*. 2003;23(1A):335–9.
55. Jiang B, Li EH, Lu YY, Jiang Q, Cui D, Jing YF, et al. Inhibition of fatty-acid synthase suppresses P-AKT and induces apoptosis in bladder cancer. *Urology*. 2012;80(2):484.e489–15.
56. Zheng SS, Gao JG, Liu ZJ, Zhang XH, Wu S, Weng BW, et al. Downregulation of fatty acid synthase complex suppresses cell migration by targeting phosphor-AKT in bladder cancer. *Mol Med Rep*. 2016;13(2):1845–50.
57. Herz J, Strickland DK. LRP: a multifunctional scavenger and signaling receptor. *J Clin Invest*. 2001;108(6):779–84.
58. Feng C, Ding G, Ding Q, Wen H. Overexpression of low density lipoprotein receptor-related protein 1 (LRP1) is associated with worsened prognosis and decreased cancer immunity in clear-cell renal cell carcinoma. *Biochem Biophys Res Commun*. 2018;503(3):1537–43.
59. Nakamura K, Urabe Y, Kagemoto K, Yuge R, Hayashi R, Ono A, et al. Genomic characterization of non-invasive differentiated-type gastric Cancer in the Japanese population. *Cancers (Basel)*. 2020;12(2):510.
60. Salama Y, Lin SY, Dhahri D, Hattori K, Heissig B. The fibrinolytic factor tPA drives LRP1-mediated melanoma growth and metastasis. *FASEB J*. 2019;33(3):3465–80.
61. Meng H, Chen G, Zhang X, Wang Z, Thomas DG, Giordano TJ, et al. Stromal LRP1 in lung adenocarcinoma predicts clinical outcome. *Clin Cancer Res*. 2011;17(8):2426–33.
62. Cao Y, Jiao N, Sun T, Ma Y, Zhang X, Chen H, et al. CXCL11 correlates with antitumor immunity and an improved prognosis in Colon Cancer. *Front Cell Dev Biol*. 2021;9:646252.

Publisher's Note

Springer Nature remains neutral with regard to jurisdictional claims in published maps and institutional affiliations.

Ready to submit your research? Choose BMC and benefit from:

- fast, convenient online submission
- thorough peer review by experienced researchers in your field
- rapid publication on acceptance
- support for research data, including large and complex data types
- gold Open Access which fosters wider collaboration and increased citations
- maximum visibility for your research: over 100M website views per year

At BMC, research is always in progress.

Learn more biomedcentral.com/submissions

